

# The effect of hybridization of fire retarded epoxy/flax-cotton fiber laminates by expanded vermiculite: Structure-property relationship study



Mateusz Barczewski <sup>a,\*</sup>, Kamila Sałasińska <sup>b,\*\*</sup>, Wojciech Raś <sup>a</sup>, Aleksander Hejna <sup>a</sup>, Sławomir Michałowski <sup>c</sup>, Paulina Kosmela <sup>d</sup>, Joanna Aniśko <sup>a</sup>, Anna Boczkowska <sup>b</sup>, Marek Szostak <sup>a</sup>

<sup>a</sup> Poznan University of Technology, Faculty of Mechanical Engineering, Institute of Materials Technology, Polymer Processing Division, Piotrowo 3, 61-138, Poznań, Poland

<sup>b</sup> Warsaw University of Technology, Faculty of Materials Science and Engineering, Wołoska 141, 02-507, Warsaw, Poland

<sup>c</sup> Cracow University of Technology, Department of Chemistry and Technology of Polymers, Warszawska 24, 31-155, Cracow, Poland

<sup>d</sup> Gdansk University of Technology, Department of Polymer Technology, Narutowicza 11/12, 80-233, Gdańsk, Poland

## ARTICLE INFO

### Article history:

Received 7 November 2022

Received in revised form

28 December 2022

Accepted 17 January 2023

### Keywords:

Epoxy resin

Composites

Hybridization

Natural fibers

Vermiculite

Flammability

## ABSTRACT

The study describes the hybridization of epoxy/flax-cotton (EP/FF) composites containing ammonium polyphosphate (APP) with micrometric expanded vermiculite (VMT) (1–10 wt%). The efficiency of hybridization of flame retarded epoxy/flax-cotton composites was assessed by performing static tensile and flexural strength evaluation, supplemented by impact strength measurements of the composites. Moreover, thermal and thermomechanical analyses (DMA, DSC, and TGA) were performed. Epoxy composites were subjected to flammability using a PCFC microcalorimeter and cone calorimetry measurement to assess the burning behavior of composites. The introduction of the low-cost plate-shaped filler resulted in several favorable thermal effects while deteriorating the structure of the composite. The addition of small amounts of vermiculite (1–2 wt%) into the matrix modified with APP enabled the reduction of heat release rate (HRR) and total heat release (THR) by 60% and 20%, respectively. The comprehensive structure-properties analysis determined the critical filler contents, yielding synergistic flame-retardant effects with a limited negative impact on the composites' performance.

© 2023 Kingfa Scientific and Technological Co. Ltd. Publishing services by Elsevier B.V. on behalf of KeAi Communications Co. Ltd. This is an open access article under the CC BY license (<http://creativecommons.org/licenses/by/4.0/>).

## 1. Introduction

Although the development of novel polymer materials groups, industrial applications' most vital emphasis is still related to modifying commonly used groups of thermoplastic and thermoset polymers aimed at improving their mechanical, thermal, thermo-mechanical, and electrical properties or reducing flammability, which significantly increases their competitiveness [1–4]. Providing new functional features to fiber-reinforced composites (FRP), carried out using hybridization by introducing powder and

particle-shaped fillers, allows for the improvement of hardness, interfacial adhesion, and impact strength [5,6]. At the same time, considering the significant attempts to increase sustainability and reduce the environmental impact, inorganic fibers, such as glass and basalt, are often replaced by natural fibers, mainly of plant origin [7–10].

Incorporating inorganic fibers increases thermal stability and may reduce the flammability of polymeric composites [11,12]; however, to achieve acceptable fire resistance, it is necessary to modify the matrix with flame retardants simultaneously. Oliwa et al. [13,14] have shown the beneficial effects of introducing antimony-free fire retardants, including ammonium polyphosphate, into epoxy laminates reinforced with glass fiber. The highest modification efficiency was noted for hybrid materials modified with multiple flame retardants or particle-shaped thermally-stable filler, yielding a synergistic effect. Reducing the

\* Corresponding author.

\*\* Corresponding author.

E-mail addresses: [mateusz.barczewski@put.poznan.pl](mailto:mateusz.barczewski@put.poznan.pl) (M. Barczewski), [kamila.salasinska@pw.edu.pl](mailto:kamila.salasinska@pw.edu.pl) (K. Sałasińska).

flammability of composites reinforced with organic fibers raises additional concerns about the deterioration of composites' flame resistance and has become an interest of various studies [15,16]. Khalili et al. [17] studied the influence of the alumina trihydrate (ATH) and ammonium polyphosphate (APP) content on the fire behavior and mechanical performance of epoxy composites reinforced with palm empty fruit bunch fibers (EFB). They showed that appropriately selected mutual concentrations (10 wt% APP/5 wt% ATH) allowed meeting the Bunsen burner test requirements while increasing the proportion of fire retardants, especially ATH, caused a significant deterioration of the mechanical properties of laminates. Similar effects were obtained for epoxy-EFB composites with expanded graphite (EG) [18]. Although a significant improvement in fire resistance, expressed by reduced dripping effects and extinguishing in the horizontal burning test, as well as a 20% reduction in gross heat during bomb calorimeter combustion, was achieved at 3 wt% of EG, a considerable strength deterioration, explained by insufficient interfacial adhesion, was also noted.

As shown in various studies [19–22], introducing inorganic particle-shaped fillers into the epoxy-laminates may improve their mechanical performance. Velmurugan et al. [22] reported that the hybridization of epoxy composites with hemp and Kevlar fibers yields a beneficial effect after adding 6 wt% of nanosilica, regardless of the reinforcing fabrics' stacking sequence. Such a relatively low filler loading caused a 10% increase in flexural and a 30% rise in tensile strength compared to laminates. While small contents of inorganic fillers can improve mechanical properties, after exceeding the critical range, the reinforcing efficiency disappears or is weakened [22]. This may result from either the increased composition viscosity or the filler agglomeration, resulting in increased amount of structural defects. Bearing in mind the phenomenon described in the literature [19] induced by the formation of Si–O–Si bonds between tourmaline nanoparticles and basalt fibers, the question arises whether the introduced inorganic particles can take an active part in changing the chemical structure of the polymer matrix. It is assumed that the beneficial effects of micro or nanometric powder fillers may be observed when the amount of filler does not exceed 5 wt% [21].

The literature also describes the effect of changing the reactivity of thermoset resins, such as epoxy and unsaturated polyesters, by incorporating the fillers [23,24]. Depending on the type of filler or its functionalization, both inhibitory and accelerating impacts on curing kinetics can be noted [23,25]. From the point of view of the production of hybrid composites, which will ultimately be characterized by high filler content, the effects of limitations in the complete curing of cast or laminated composites require special attention. Zhao and Drummer [24] reported modification in curing kinetics of powdered epoxy resin modified by glass beads and hydrophobic fumed silica. Based on the analysis related to Kamal-Sourour model, the authors showed that the introduction of glass beads to epoxy monomer resulted in inhibition in cross-linking of epoxy resin in a three-dimensional direction, resulting from reduced space for the resin reaction in composite bulk. Other studies confirm that immobilization of the monomers or partially cured fractions of the resin, its limited dispersion, and partial reactivity of chemical groups on the filler surface with monomer or curing agents in the highly-filled composition are usually the main effect in inhibitory behavior during thermoset composite production [24,26]. Therefore, every time the hybridization of reactive thermoset polymers-based laminates with inorganic fillers is undertaken, it is essential to consider the possibilities of the occurrence of complex structural interactions.

Reducing the flammability of natural composites requires the suitable content of fire retardants; however, the high share is not indifferent to the strength of the final products. Therefore, it is necessary to focus on determining compositions that maximize the

effectiveness of components' mutual interactions. In this study, attempts were made to introduce into the epoxy matrix various concentrations of plate-shaped filler in the form of expanded and shredded vermiculite simultaneously with ammonium polyphosphate (APP) as an intumescent flame retardant. Hybrid epoxy compositions with a high degree of filling were used as a matrix to produce layered composites reinforced with flax-cotton fibers. The work presents an in-depth analysis of changes in the reactivity of the thermoset system, correlating the observed changes with the modification of thermomechanical properties and the flammability of laminates.

## 2. Experimental

### 2.1. Materials and sample preparation

The polymeric matrix was epoxy resin based on bisphenol A diglycidyl ether, Epidian 652 (EP, density 1.10 g/cm<sup>3</sup>, epoxy number 0.48–0.51 mol/100 g and viscosity 500–900 mPa·s at 25 °C) and isophorone diamine, IDA (amine number 200–350 mg KOH/g and viscosity 150–300 mPa·s at 25 °C) from CIECH Sarzyna S.A [27].

Commercially available intumescent flame retardant ammonium polyphosphate (APP), Exolit AP 422 from Clariant, was applied in the presented study [28].

Vermiculite (VMT) from Perlit Polska was delivered in thermally expanded form. Its annealing process was carried out at 1260 °C. The pre-processing of the filler included milling in a Retsch ZM 200 high-speed grinder at 10 000 rpm and sieving with a 50 µm sieve by Fritsch Analysette 3 Pro apparatus. The chemical composition, according to the manufacturer's data, is 38.0–49.0% SiO<sub>2</sub>, 20.0–23.5% MgO, 12.0–17.5% Al<sub>2</sub>O<sub>3</sub>, 0.3–5.4% Fe<sub>2</sub>O<sub>3</sub>, 5.2–7.9% K<sub>2</sub>O, 0.0–1.2% FeO, 0.7–1.5% CaO, 0.0–0.8% Na<sub>2</sub>O, 0.0–1.5% TiO<sub>2</sub>, 0.0–0.5 Cr<sub>2</sub>O<sub>3</sub>, 0.1–0.3% MnO, 0.0–0.6% Cl, 0.0–0.6% CO<sub>2</sub>, 0.0–0.2% S. Applied VMT filler was characterized with the density of 2.61 g/cm<sup>3</sup>, and 12.58 m<sup>2</sup>/g BET surface area. Broader information about the used filler was presented in previous works [29–31].

As a reinforcing filler, flax-cotton woven fabrics (FF) with a 56:44 flax-to-cotton ratio and a plain weave, grammage of 160 g/m<sup>2</sup>, and 5% shrinkage (Polski Len, Poland) were used [32].

The epoxy monomer-APP-VMT compositions were prepared by mechanical mixing using a ProLAB Disperlux stirrer equipped with a disc agitator at 3000 rpm for 10 min under subatmospheric pressure (0.2 bar). After degassing, the IDA curing agent was introduced, and the composition was stirred again at 1000 rpm for 3 min. The constant resin-to-curing agent ratio (100:50 by weight) was used. Before manufacturing, the fabrics, APP, and VMT were dried using Memmert ULE 500 cabinet dryer for 48 h at 50 °C. The seven-layer laminates were prepared using 350 × 350 mm sheets of fabric by hand lay-up method. After the forming process, without application of the clamping pressure after the fiber-saturation process, samples were cured at ambient temperature for 168 h and post-cured for the next 72 h at 80 °C using Memmert ULE 500 cabinet dryer. The final thickness of the individual laminate series was as follows: EP/FF (3.47 ± 0.09 mm), EP/FF/APP (4.29 ± 0.14 mm), EP/FF/APP/1VMT (4.33 ± 0.42 mm), EP/FF/APP/2VMT (4.69 ± 0.21 mm), EP/FF/APP/5VMT (4.11 ± 0.39 mm), EP/FF/APP/10VMT (4.60 ± 0.26 mm). The procedure for manufacturing the laminates is presented as a graphic diagram in Supplementary Information in Fig. S1. An explanation of the sample assignment, the molding technique's specification, and the content of individual components is included in Table 1.

### 2.2. Methods

The viscosities of the epoxy compositions filled with various amounts of VMT were determined using a rotational rheometer

**Table 1**  
Sample assignment and compositions.

Sample assignment	Epidian	APP	VMT	Flax-cotton	Manufacturing method
	652: IDA; [ratio; wt%]	[wt%]	[wt%]	fabrics [ + / - ]	
EP	100:50; 100	0	0	–	casting
EP/APP	100:50; 80	20	0	–	
EP/APP/1VMT	100:50; 79	20	1	–	
EP/APP/2VMT	100:50; 78	20	2	–	
EP/APP/5VMT	100:50; 75	20	5	–	
EP/APP/10VMT	100:50; 70	20	10	–	
EP/FF	100:50; 100	0	0	+	Hand-lay-up lamination
EP/FF/APP	100:50; 80	20	0	+	
EP/FF/APP/1VMT	100:50; 79	20	1	+	
EP/FF/APP/2VMT	100:50; 78	20	2	+	
EP/FF/APP/5VMT	100:50; 75	20	5	+	
EP/FF/APP/10VMT	100:50; 70	20	10	+	

Anton Paar MCR 301 operated with a 25 mm parallel plates measuring system with a gap of 0.3 mm. All specimens were pre-sheared before testing for 1 min with a shear rate of  $1 \text{ s}^{-1}$  and a subsequent relaxation time of 1 min. The measurements were realized in constant shear mode using  $5 \text{ s}^{-1}$  shear rate at  $30^\circ\text{C}$ . The presented dynamic viscosity results are mean values from the 300 s experiment.

The Fourier transform infrared spectroscopy (FTIR) measurements were realized using a spectrometer Jasco FT/IR-4600 at room temperature ( $23^\circ\text{C}$ ) and in a mode of Attenuated Total Reflectance (ATR - FT-IR). Sixty-four scans at a resolution of  $4 \text{ cm}^{-1}$  were used in all cases to record the spectra.

Differential scanning calorimetry (DSC) measurements were carried out using a Netzsch DSC 204F1 Phoenix apparatus from Netzsch GmbH, in reference to ISO 11357 standard [33]. Material samples of  $10 \pm 0.1 \text{ mg}$  were placed in aluminum crucibles with pierced lids, then heated and cooled at a temperature from  $0^\circ\text{C}$  to  $160^\circ\text{C}$  in a nitrogen atmosphere at a heating/cooling rate of  $10^\circ\text{C}/\text{min}$ .

The thermal properties of epoxy and its' composites filled with various amounts of VMT in the form of castings and laminates with natural fibers were determined by thermogravimetric analysis (TGA) with the temperature set between  $30^\circ\text{C}$  and  $900^\circ\text{C}$  at a heating rate of  $10^\circ\text{C}/\text{min}$  and under nitrogen atmospheres, using a TG 209 F1 Netzsch apparatus, according to ISO 11358 standard [34]. Samples of  $10 \pm 0.2 \text{ mg}$  were placed in ceramic pans. The initial decomposition temperature was determined as the temperature of 5 wt% mass loss ( $T_{5\%}$ ), while the residual mass ( $\Delta W\%$ ) was at  $900^\circ\text{C}$ .

The analysis of the combustion process of epoxy composites was carried out using a Pyrolysis Combustion Flow Calorimeter (PCFC) manufactured by Fire Testing Technology Ltd, in reference to ASTM D 7309 standard [35]. The sample was first heated at a constant rate of  $1^\circ\text{C}/\text{s}$  in a pyrolyzer. The thermal decomposition products were swept from the pyrolyzer by an inert gas. After pyrolysis, the gas stream was mixed with oxygen and entered a combustor at  $900^\circ\text{C}$ , where products are completely oxidized following decomposition. Oxygen concentrations and flow rates of the combustion gases were used to determine the oxygen depletion involved in the combustion process, the heat release, and the heat release capacity. The samples tested had masses of  $1.6 \pm 0.4 \text{ mg}$ .

Burning behavior was assessed by cone calorimeter tests conducted on Fire Testing Technology apparatus following the ISO 5660–1 and ISO 5660–2 procedures [36]. The horizontally oriented cuboid specimens, with dimensions of  $100 \times 100 \times 4 \text{ mm}$ , were irradiated at a heat flux of  $50 \text{ kW}/\text{m}^2$ . Spark ignition was used to ignite the pyrolysis products. An optical system with a silicon photodiode and a helium-neon laser provided a continuous survey

of smoke. The residue after tests was photographed using a digital camera.

The dynamic mechanical-thermal analysis (DMA) was conducted in torsion mode using Anton Paar MCR 301 rheometer with an SRF measuring system in reference to ISO 6721 standard [37]. Investigations were carried out with a constant frequency of 1 Hz and a strain of 0.01%. The measurements were realized in a temperature range of  $30\text{--}200^\circ\text{C}$  with a  $3^\circ\text{C}/\text{min}$  temperature ramp for samples in the form of castings with various VMT amounts and laminates manufactured with their use.

The mechanical behavior of the composites was investigated using static tensile and flexural tests. The tensile and flexural tests were performed according to ISO 527 [38,39] and ISO 178 [40] standards with a Zwick/Roell Z020 universal testing machine at room temperature. The elastic modulus measurements were conducted at a crosshead speed of 1 mm/min, while the elongation at the break at 5 mm/min. Flexural strength measurements were realized with a crosshead speed of 1 mm/min during the evaluation of the bending modulus and 1.5 mm/min over the remaining parts of the experiment. The number of samples measured was 10.

Hardness was evaluated using the Sauter HBD 100-0 Shore D durometer according to ISO 868 standard [41]. The presented test results are the mean value of 30 measurements taken for each composite series.

The impact strength of the unnotched samples was examined by the Charpy method according to ISO 179 [42], and the peak load was determined as the maximum force ( $F_{\text{max}}$ ). The Zwick/Roell HIT 25 P impact tester with a 5-J hammer was applied for the measurement. The number of samples measured was 10.

### 3. Results and discussion

#### 3.1. Rheological assessment of epoxy compositions

The filler content and its physicochemical properties may strongly influence thermoset polymers' rheological and curing behavior [43]. Therefore, the characterization of compositions containing curing agents before forming was undertaken. Fig. 1 summarizes the results of rheological measurements made for the epoxy composition with the hardener after introducing 20 wt% of APP and variable VMT content. Many factors influence particle suspensions' rheological properties, including the particles' geometry resulting from particle pre-processing [44]. The addition of APP caused a two-fold increase in viscosity compared to EP. The additional introduction of VMT in lower amounts (1–5 wt%)

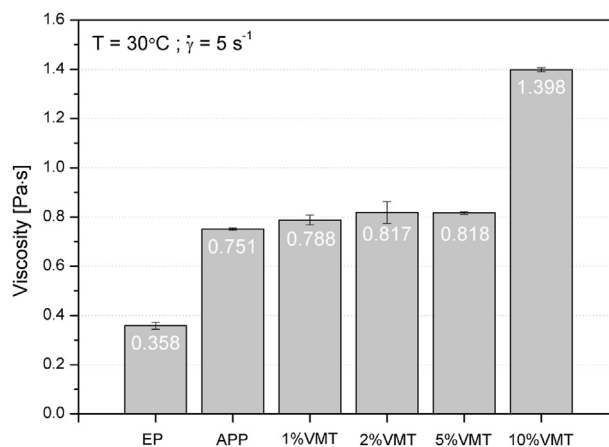


**Fig. 1.** Viscosity of EP-based compositions with various amounts of VMT.

resulted in a comparable increase in viscosity. While individual series gradually show higher viscosity with an increasing share of the inorganic filler, it can be concluded that adding up to 5 wt% of VMT into epoxy composition with 20 wt% APP content did not deteriorate the rheological properties significantly. A substantial increase in viscosity was noted in the case of a composite containing 10 wt% of the VMT. EP/APP/10VMT composition is characterized by twice as high viscosity as EP-APP and almost five times higher than unmodified epoxy resin. Taking into account the previous studies [45], it can be concluded that the viscosity at the recorded level should also not be a significant problem during molding, both for castings and laminate molding by hand lay-up or vacuum bagging method.

### 3.2. Spectroscopic structure evaluation

Fig. 2 shows the FTIR spectra of unmodified and modified with APP epoxy resin and their composites with various content of the VMT, after curing, formed as castings and laminates reinforced with natural fibers. The measurements were taken for samples cured in the same procedure, including the post-curing. The spectra of epoxy resin consist of the most distinct absorbance bands for this polymer at 3365  $\text{cm}^{-1}$  (O–H stretching), 2965–2852  $\text{cm}^{-1}$  (stretching C–H of  $\text{CH}_2$  and CH aromatic and aliphatic), 1728  $\text{cm}^{-1}$  (C=O from benzyl methyl ketone), 1609  $\text{cm}^{-1}$  (C=C aromatic ring stretching), 1509  $\text{cm}^{-1}$  (C–C stretching of aromatic ring), 1180  $\text{cm}^{-1}$  (C–O aromatic ring stretching), 1112–1190  $\text{cm}^{-1}$

(broad overlapping of aromatic stretching and C–O aromatic ring stretching), 1032  $\text{cm}^{-1}$  (stretching of C–O–C ethers), 830  $\text{cm}^{-1}$  (C–O–C of oxirane group, aromatic absorbance), and 722  $\text{cm}^{-1}$  (rocking  $\text{CH}_2$ ) [46–48]. Unmodified VMT usually reveals several absorption bands characteristic of its structure at 3355  $\text{cm}^{-1}$  (assigned to O–H stretching vibration), as well as 957, 671, and 460  $\text{cm}^{-1}$  (respectively from Si–O, Al–O, and Mg–O lattice vibrations) [49–51]. The band at 957  $\text{cm}^{-1}$  may be observed for composites containing VMT; however, its intensity is independent of the filler content, resulting from the lower amount of the filler on the surface of the sample. The additional bands characteristic of APP [52], especially in the O–H vibration band range, were noted for samples containing fire retardant. The addition of hydrophilic APP caused a shift of the overlapping O–H and N–H vibration bands peak to higher wavelengths. In the case of DGEBA-based epoxy resins, various peaks are used to determine the curing process, such as 760, 915, and 970  $\text{cm}^{-1}$ . The lack of signal at 915  $\text{cm}^{-1}$  from C–O oxirane stretching suggests proper curing process realization [53]. The presence of an 830  $\text{cm}^{-1}$  band resulting from *p*-phenylene groups visible at spectra has not varied significantly in their intensity, and according to Fraga [53], they should not be used to assess the curing process and its' kinetics. FTIR spectra of reinforced composites (Fig. 2 b,d) vary from those obtained for castings (Fig. 2 a,c). The main difference is a significant reduction of the absorbance band of O–H stretching and the presence of a distinct peak at 867  $\text{cm}^{-1}$  reflecting C–O deformation vibrations [54]. According to the mechanism proposed by Maity et al. [55], observed

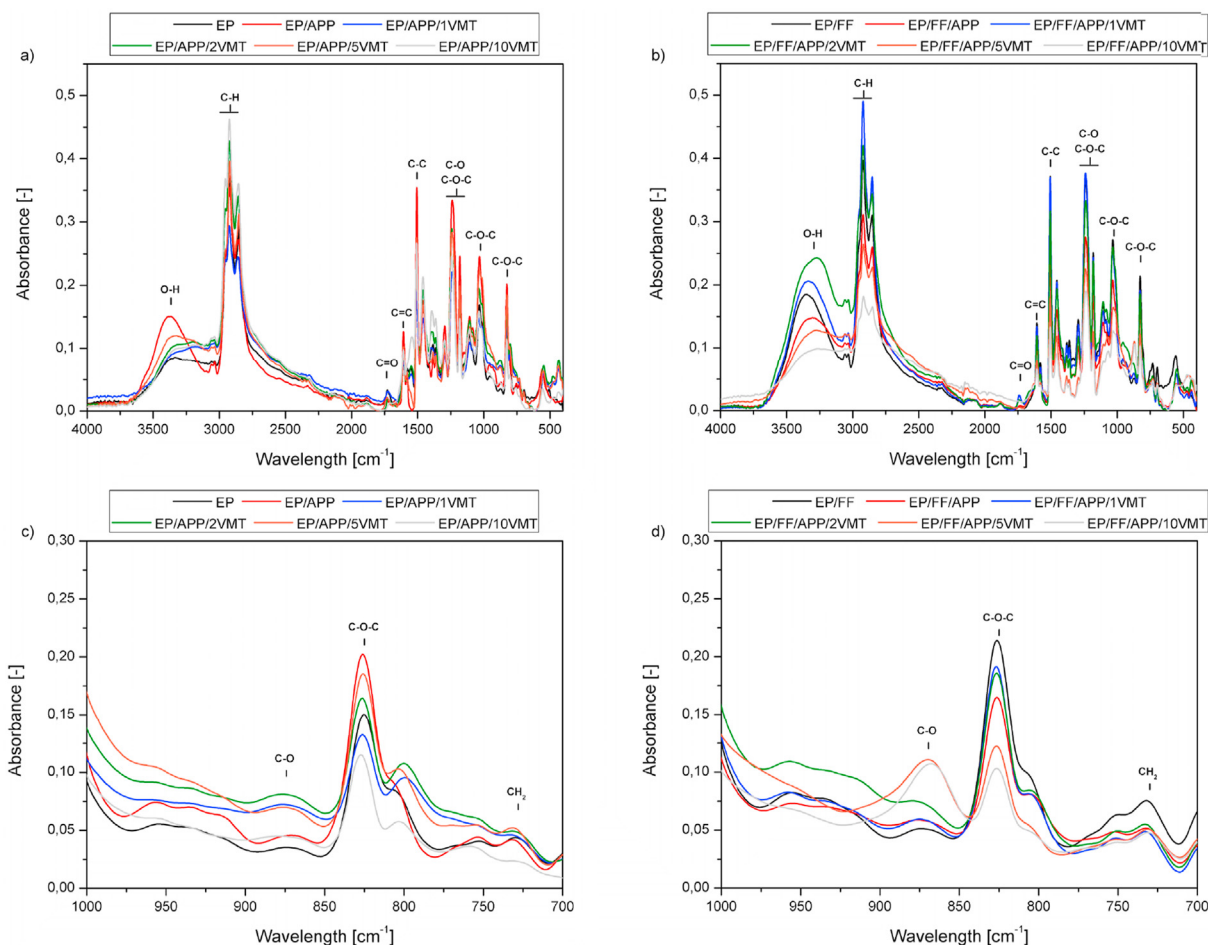


Fig. 2. FTIR spectra of non-reinforced (a,c) and reinforced with natural fibers (b,d) EP and EP-based composites in the range of 4000–400  $\text{cm}^{-1}$  and 1000–700  $\text{cm}^{-1}$ .

changes in FTIR spectra may suggest the composition's reactivity changes by potential hydrogen bonding between natural fibers' free surface hydroxyl groups and epoxy matrix. As a result, the natural filler bonded with the polymeric matrix, decreasing the cross-link density of fiber-reinforced composites containing over 2 wt% of VMT due to the lack of proper stoichiometric adjustments during the manufacturing process.

### 3.3. Differential scanning calorimetry (DSC)

DSC analysis was performed to indirectly assess the correct course of the cross-linking process and describe the influence of interactions between the components in the complex flame retardant composite system. The tests were carried out for composites without and with the presence of a fibrous filler. This procedure provides information about the potential effects of APP, VMT, and FF addition on the cross-linking of final products, as a supplementary to FTIR spectroscopic analysis. In the case of DSC analysis, obtained value can be a criterion for assessing changes in the degree of cross-linking or phase separation phenomena in composites [56,57]. Fig. 3 shows the DSC thermograms of epoxy samples containing APP and various contents of VMT. The glass transition temperature determined by DSC ( $T_{gDSC}$ ) as an inflection determined from the first derivative of the heat flow curve for castings/laminates was as follows: EP (49.3 °C/50.6 °C), APP (53.2 °C/58.5 °C), EP/APP/1VMT (55.4 °C/57.4 °C), EP/APP/2VMT (53.8 °C/59.3 °C), EP/APP/5VMT (54.2 °C/60.0 °C), EP/APP/10VMT (60.5 °C/51.2 °C).

With the increasing content of the filler, the glass transition temperature gradually increases, except EP/APP/FF/10VMT series. This effect is related to the interactions between the epoxy resin and active surfaces of micrometric inorganic filler domains. According to Papanicolaou et al. [58], higher  $T_g$  values are related to the increasing interphase volume, which implicates a higher share of interfacial defects. No exothermic processes in the range above the  $T_{gDSC}$  were noted in any DSC curves, indicating that the composition was completely cured. The higher cross-link density usually decreases the mobility of macromolecules at higher temperatures. It can be concluded that neither the fire retardant nor the inorganic filler inhibited the cross-linking process, understood as a limitation in unreacted groups mobilization in the polymer bulk caused by phase separation of the components. Increased  $T_{gDSC}$  characterized compositions containing both APP and fine-dispersion VMT, which can be attributed to the hindering of the macromolecular chains' motions by high-surface area filler. The intermolecular interactions between epoxy and VMT may also result from hydrogen bonding between hydroxyl groups of epoxy

and functional groups present on the filler's surface [59], limiting the macromolecular motions at elevated temperatures [60]. Structural changes observed by FTIR for EP/FF/APP/10VMT series have been confirmed by DSC, suggesting reduced cross-link density in polymeric bulk caused by interfacial interactions induced by a high content of particle-shaped modifiers and fillers.

### 3.4. Thermomechanical and mechanical properties

Fig. 4 shows the thermomechanical curves in the form of storage modulus ( $G'$ ) and damping factor ( $\tan \delta$ ) vs. temperature plots for epoxy composites containing APP, and VMT, with and without the presence of natural fibers. In addition, the thermomechanical parameters obtained during DMA are summarized in Table 2. It shows the  $G'$  values at 30, 80, and 120 °C, corresponding to the values below and above the  $\alpha$ -relaxation of epoxy resin range, as well as 120 °C, the temperature after stabilization of changes in thermomechanical properties, which can constitute the maximum operating temperature of the potential product. The values of the glass transition temperature  $T_{gDMA}$  marked as the maximum on the  $\tan \delta$  curve were also given, along with the corresponding values of the damping factor.

The highest stiffness at ambient and elevated temperatures was observed for the APP-modified composite reinforced with natural fibers containing 1 and 2 wt% of VMT. The storage modulus values can be compared with changes in elasticity modulus determined by the static tensile test [61]. At the same time, a different measuring system and a greater complexity of interactions during dynamic non-destructive tests provide much more information about the sample structure [62]. As in the case of static mechanical tests, the introduction of 5 and 10 wt% of VMT into fiber-reinforced laminates reduced the materials' stiffness, for castings deterioration of storage modulus was noted only for composites containing 10 wt% of the VMT, resulting from phase separation or inorganic filler agglomeration. Moreover, the observed increase in  $T_{gDMA}$  with the simultaneous increase in  $G'$  for the composition containing APP and APP along with 1 and 2 wt% of VMT points to good interfacial adhesion [60,63,64]. The  $G'$  also quantifies the elastic energy stored by the material. A simultaneous increase in both thermomechanical parameters indicates enhancement of chemical and physical interactions between the polymer and the filler, associated with reduced mobility of epoxy matrix macromolecules in the composite [65]. A further increase in the filler fraction decreased  $T_{gDMA}$ . The castings showed lowered peak values of  $\tan \delta$ , pointing to the reinforcing ability of the inorganic particle-shaped filler [66]. Higher  $\tan \delta$  values may be associated with the enhanced damping

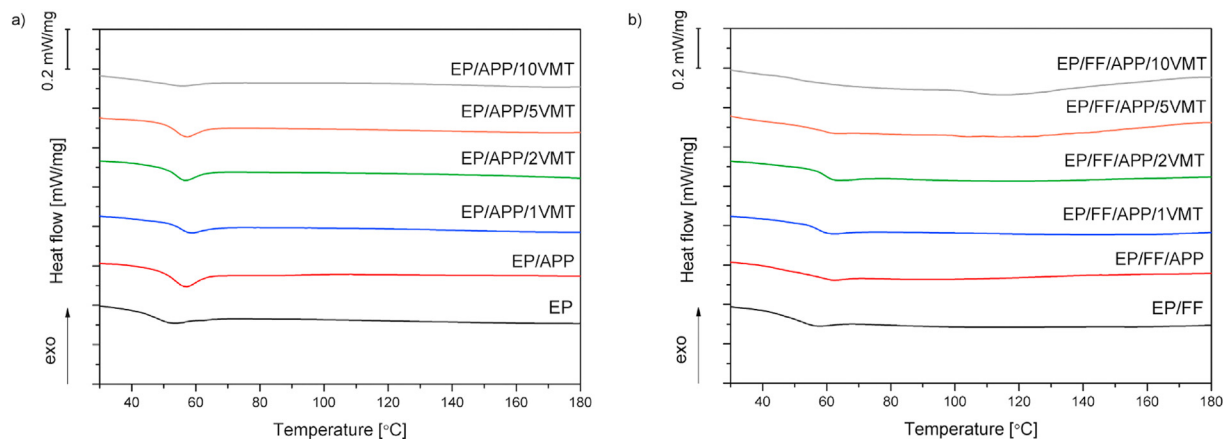


Fig. 3. DSC heating thermograms obtained for non-modified EP, fire retarded EP-APP, and their composites of castings (a) and natural fiber-reinforced laminates (b).

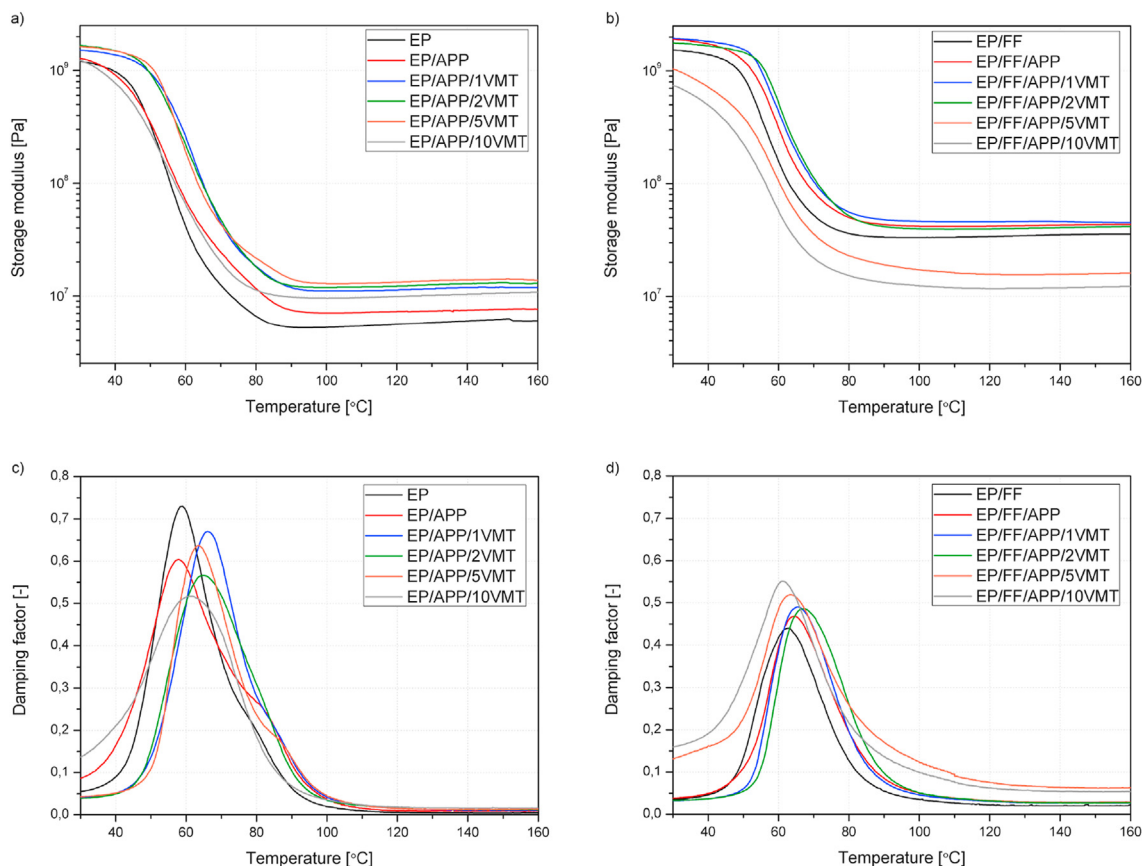


Fig. 4. Storage modulus and damping factor vs. temperature of EP composites without (a,c) and reinforced with natural fibers (b,d).

ability of the composites containing natural fibers. However, this phenomenon can also be attributed to interphase imperfections, e.g., porosity from inefficient degassing of the composition containing fillers and fire retardant. The differences between  $T_g$  values obtained from DSC and DMA are due to much more complex information contained during DMA analysis. The  $T_g$  determined as the local maximum of relaxation phenomena in the thermo-mechanical analysis is influenced not only by macromolecular interactions as in DSC but is 'distorted' by interfacial effects and structural defects in the tested sample [67].

It should be emphasized that no storage modulus increase was noted, which could be attributed to the post-curing processes. Despite the unchanged stoichiometry of the epoxy monomer-

amine curing agent system, its reactivity changed due to the interactions with the fibrous filler and phase separation during forming and curing of the laminates. It may cause local variations in the cross-linking density distribution affecting the composites' performance [68]. Considering increasing viscosity, there is a risk of phase separation and the creation of clusters. Moreover, interfacial side reactions may occur while heating and mixing a high-viscosity composition containing particle-shaped fillers. To summarize, applying APP and low amounts of VMT in fiber-reinforced and casting composites enhanced stiffness at elevated temperatures.

The effect of the hybridization of prepared composites by expanded vermiculite was assessed in terms of static (tensile and flexural tests) and dynamic (Charpy impact strength) mechanical load and Shore D hardness. The results for composites manufactured with a constant APP content and a variable amount of VMT are summarized collectively in Fig. 5 and Supplementary Information in Table S1. Similar behavior resulting from the APP incorporation was noted for both tests performed under static load conditions. The tensile and flexural strength decreased by 14.8 and 12.1 MPa, respectively, 27% lower than unmodified EP in both cases. The results are in line with former studies. Wang et al. [69] reported a similar decrease in the mechanical performance of epoxy composites reinforced with ramie fibers after adding 20 wt% of APP.

The addition of VMT into the composite structure resulted in similar behavior, i.e., with filler content up to 2 wt%, the tensile and flexural strength increased compared to a composite containing 20 wt% of APP. The flexural strength enhancement was more significant, and composites containing 1 and 2 wt% of VMT had more than twice the flexural strength of the EP/FF/APP revealing the

Table 2

Thermomechanical parameters of EP composites obtained by DMA.

Sample	Storage modulus, $G'$ [Pa]			$T_{g,DMA}$ [°C]	$\tan \delta$ [-]
	30 °C	80 °C	120 °C		
EP	$1.20 \cdot 10^9$	$6.53 \cdot 10^6$	$5.58 \cdot 10^6$	59.0	0.70
EP/APP	$1.28 \cdot 10^9$	$1.16 \cdot 10^7$	$7.24 \cdot 10^6$	57.9	0.61
EP/APP/1VMT	$1.52 \cdot 10^9$	$1.82 \cdot 10^7$	$1.13 \cdot 10^7$	66.1	0.67
EP/APP/2VMT	$1.66 \cdot 10^9$	$1.80 \cdot 10^7$	$1.22 \cdot 10^7$	65.1	0.57
EP/APP/5VMT	$1.63 \cdot 10^9$	$2.16 \cdot 10^7$	$1.33 \cdot 10^7$	63.6	0.64
EP/APP/10VMT	$1.23 \cdot 10^9$	$1.13 \cdot 10^7$	$9.86 \cdot 10^6$	61.3	0.52
EP/FF	$1.54 \cdot 10^9$	$3.60 \cdot 10^7$	$3.39 \cdot 10^7$	63.0	0.44
EP/FF/APP	$1.91 \cdot 10^9$	$4.99 \cdot 10^7$	$4.18 \cdot 10^7$	64.2	0.47
EP/FF/APP/1VMT	$1.94 \cdot 10^9$	$5.57 \cdot 10^7$	$4.59 \cdot 10^7$	65.2	0.49
EP/FF/APP/2VMT	$1.77 \cdot 10^9$	$5.16 \cdot 10^7$	$3.95 \cdot 10^7$	66.6	0.49
EP/FF/APP/5VMT	$1.04 \cdot 10^9$	$2.30 \cdot 10^7$	$1.57 \cdot 10^7$	63.2	0.52
EP/FF/APP/10VMT	$7.43 \cdot 10^8$	$1.53 \cdot 10^7$	$1.17 \cdot 10^7$	60.8	0.55

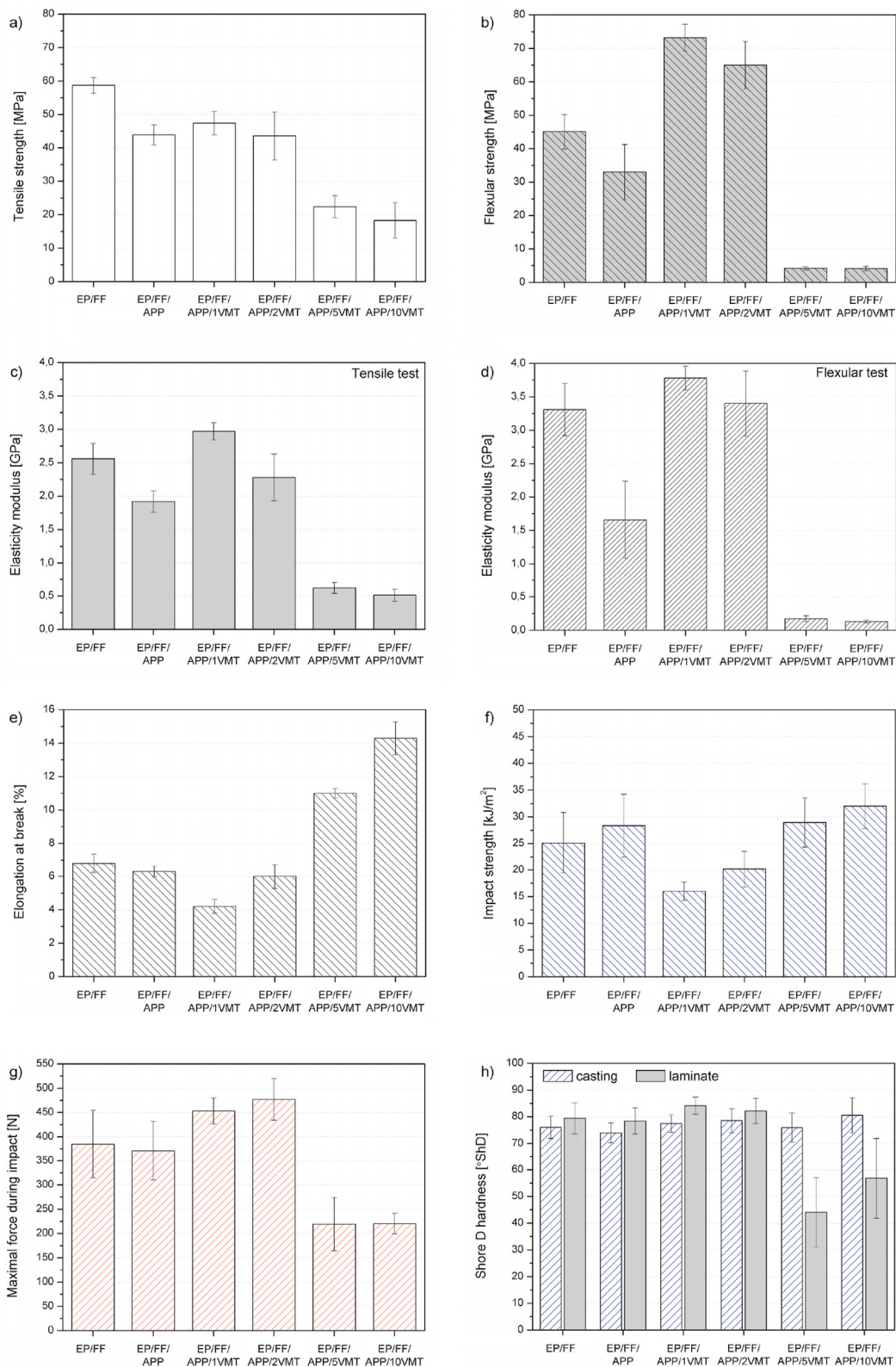


Fig. 5. Mechanical behavior of natural fiber reinforced epoxy composites; tensile test (a, c, e), flexural test (b, d); Charpy impact strength (f, g), Shore D hardness (h).

best mechanical performance in terms of flexural strength. Srinivasan and co-workers reported a similar effect of flexural strength improvement [70] after incorporating 3 wt% of  $\text{CaCO}_3$  into banana fiber-reinforced epoxy composites. A further increase in the

amount of VMT resulted in a drastic reduction in both tensile and flexural strength. Changes in the composites' stiffness due to additives and fillers were mirrored in the case of tensile and flexural strength; however, introducing 1 wt% of VMT enabled obtaining

the highest stiffness and limiting the strength deterioration caused by APP. Materials containing 5 and 10 wt% of the filler showed negligible stiffness excluding them from being used as construction materials. The elongation at break of EP/FF/APP/5VMT and 10VMT samples pointed to the plasticization of the polymeric matrix and decreased interfacial adhesion. Usually, in the case of composites modified with long fibers, the modification of the matrix by adding particulate insoluble modifiers or fillers leads to significant changes in elongation at break (its depression) [5,70,71] because the fibers themselves have a dominant share in the stress transmission. In the considered case, structural changes of the EP/APP/VMT system with 5 and 10 wt% of VMT limited the possibility of effective stress transmission by fibers due to the significantly softened matrix. These results are in line with the storage modulus changes reported by the DMA. During the cross-linking process, considering the disappearance of oxirane groups, the consumption of reactive groups yielded a stable chemical and physical state of the material [72]. On the other hand, changed viscosity may affect the reactivity of the monomer-filler, hardener, and filler systems. Simultaneously, higher viscosity induced by the presence of VMT may impede the mixing process and, along with enhanced interfacial interactions between the inorganic filler and polymer matrix, reduce the network mobility limiting further reactions [72].

Charpy impact resistance is inversely proportional to the results of composite stiffness. Stiffened by the presence of 1 and 2 wt% VMT, fiber-reinforced composites showed the lowest impact resistance. Despite the introduction of significant amounts of powder fillers, the modification of the structure of the polymer matrix eliminated the adverse impact of rigid VMT domains. Thus, the increase in impact toughness resulting from the introduction of 5 and 10 wt% of the filler did not come from the enhanced interfacial interactions described in the literature [73] but from the improved impact resistance of the polymer matrix itself. On the other hand, this effect was observed for compositions with the lowest proportion of VMT, which probably did not limit the suspensibility of the system and did not enhance the interactions with the reactive polymer matrix, and acted on internal notches in the structure of dynamically loaded composites [74]. During dynamic destructive loads of fiber-reinforced composites, a complicated simultaneous mechanism usually occurs: polymer matrix cracking, fiber-matrix debonding, delamination, and fiber pull-out [75]. It should be mentioned that the introduction of rigid filler domains into fabric-reinforced composites, in the absence of significant structural changes in the polymer matrix and proper adhesion at the fiber-filler interface, increases the delamination area at the point of impact, which results in increased impact resistance [76]. In the case of composites with high VMT content (5 and 10 wt%), no delamination phenomenon was noted during the impact, and improved durability resulted from the decreased elasticity of the matrix.

The composites' hardness (Fig. 5h) was tested for samples in the form of castings and laminates made with flax-cotton fibers. In the case of castings, no significant changes in the hardness were noted, while the laminates containing APP only and the lowest concentrations of VMT were characterized by increased hardness. The unfavorable plasticization effects of the polymer matrix caused by the introduction of 5 and 10 wt% of VMT reduced hardness by almost 50% compared to the casting. Considering that the hardness of the thermoset polymers may be related to cross-linking density [56,77], observed changes are in good agreement with the structural analysis realized by DSC and FTIR.

### 3.5. Thermal stability and flammability

#### 3.5.1. Thermogravimetric analysis (TGA)

Thermogravimetric analysis on the components, EP, and samples with different content of VMT and epoxy laminates were conducted to study the influence of the fillers on thermal degradation. The TG and DTG are depicted in Fig. 6, and the decomposition temperatures at 5% mass loss (T<sub>5%</sub>), rate of decomposition in each step (DTG1–DTG3), and the residue at 900 °C are summarized in Table 3.

All samples showed a thermally induced and temperature-dependent degradation [16]. The 5% mass loss, corresponding to the thermal decomposition onset, for unmodified epoxy resin reached 174 °C and was reduced only in the case of EP/FF. Although a slight peak was observed on DTG curves around 200 °C, the most intense degradation of EP, related to the decomposition of the aromatic group of the resin and the aliphatic amine from the curing agent, appeared above 300 °C [78]. The decomposition of the applied components overlapped with the degradation of epoxy resin, causing at the same time a shift of peaks towards lower temperatures; however, the rates of decomposition of composites, especially FF/APP/VMT series, were similar or lower compared to EP, which could be attributed to the reduced matrix share. The residual mass of laminates was almost three times higher than the unmodified EP, increasing with the VMT content. The lack of a linear relationship can be attributed to the small size of the samples used for the TG analysis. Improving the char formation ability is beneficial from a fire hazard point of view. It can be concluded that the combination of APP, FF and VMT caused an increase in the T<sub>5%</sub>, a decrease in the decomposition rate, and accompanying growth in the char yield.

#### 3.5.2. Pyrolysis combustion flow calorimetry

Pyrolysis combustion flow calorimetry (PCFC) is an analytical technique for evaluating milligram-sized samples' flammability. The equipment aims to reproduce the processes that occur while burning but without maintaining a flame [79]. Since the research was carried out with the use of the PCFC, the critical parameters for the EP and samples with different content of VMT, such as heat release rate (HRR) in the form of a peak (pHRR), temperature (T<sub>pHRR</sub>) of occurrence of pHRR, the total heat release (THR) and heat release capacity (HRC), were determined. The course of the heat release rate of individual materials is shown in Fig. 7. Table 4 presents the parameters of the combustion process of each material, considering standard deviations from the average value.

As can be seen from Fig. 7, the thermal degradation process occurred in several stages, with a heat release in each of them [80]. In 310 and 350 s, two peaks characterized the HRR curve course of EP, while the resin samples with VMT had from two to four HRR peaks, the first yielding the pHRR. All composites, except EP/APP/2VMT (329 W/g), had an equal to or higher value than that obtained for the unmodified resin, and the highest was noted for EP with a commercial flame retardant. Moreover, the addition of APP shifted the T<sub>pHRR</sub> towards lower temperatures than EP, similar to TGA results (DTG 2).

The highest value of total heat release was noted for EP (33.8 kJ/g), while the addition of commercial flame retardant caused a reduction of 30%. Moreover, the combination of APP with VMT led to a further decrease in THR, and the lowest values were obtained for EP/APP/10VMT (20.7 kJ/g). The heat release capacity is one of the most approved indicators to assess the fire hazard of materials [79]. The HRC of EP was 385 J/gK, and only for EP/APP/1VMT and EP/



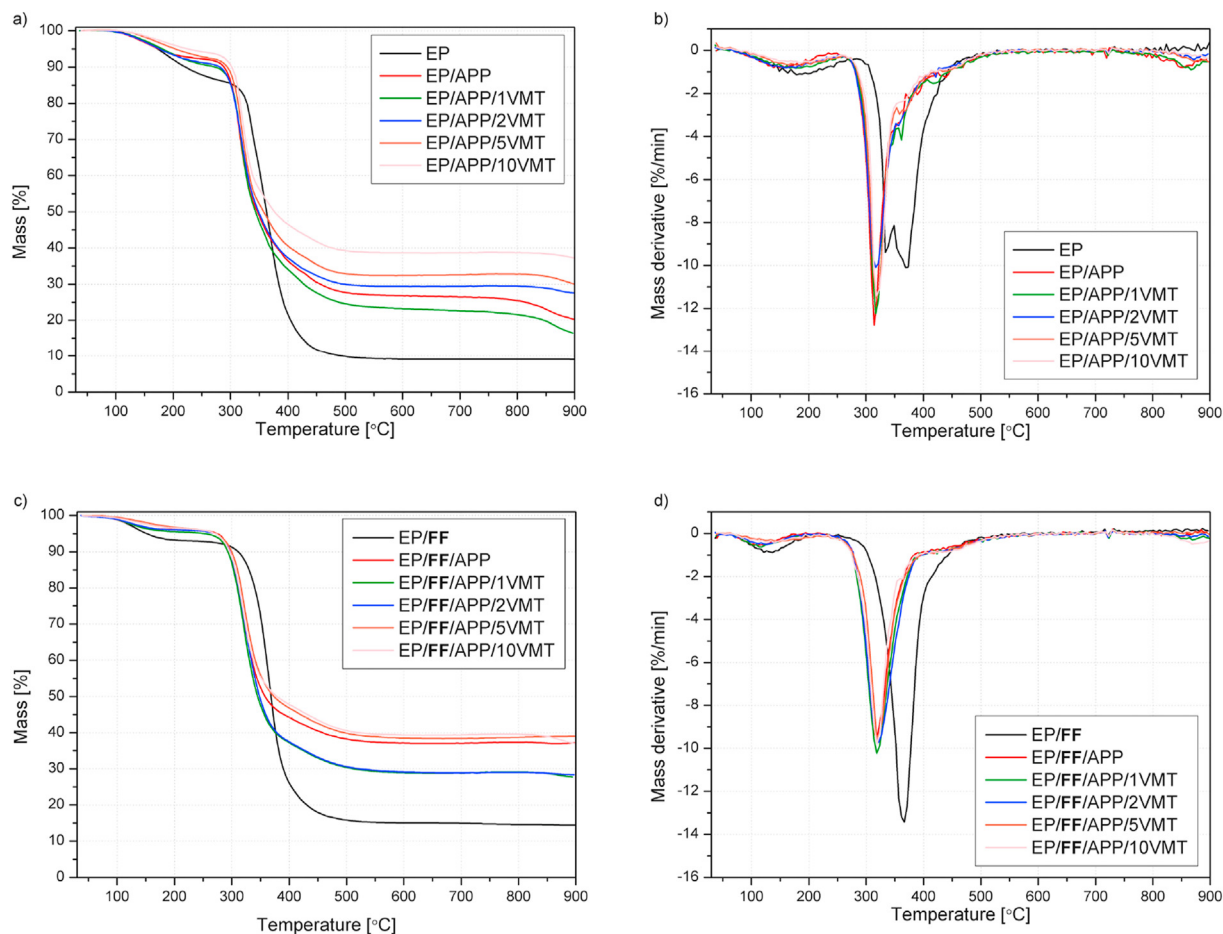


Fig. 6. TG and DTG curves of samples with various content of VMT (a, b), and epoxy laminates (c, d).

APP/2VMT similar or lower values were observed. The lowest HRC was obtained in the case of EP containing 2 wt% VMT, and the value was lower even than for EP/APP/5VMT and EP/APP/10VMT. It can be concluded that the simultaneous incorporation of APP and VMT can improve the flame resistance of epoxy; however, the amount of VMT should be less than 2%. Similarly, the highest HRC was

obtained for a resin containing only a commercial flame retardant (470 J/gK). A disadvantage of PCFC is that some of the significant flame-retardation mechanisms, including barrier effects and flame inhibition/radical scavenging, are not considered adequately due to the small sample size and forced complete combustion of the volatiles [79]. Although it is not an appropriate screening tool for

Table 3  
TGA thermal parameters of components, samples with various content of VMT and epoxy laminates.

Sample	T <sub>5%</sub> [°C]	DTG 1 [°C; %/min]	DTG 2	DTG 3	DTG 4	Residual mass [%]
<b>Fillers</b>						
APP	317	–	305; –1.72	–	560; –1.90	64.18
VMT	–	–	–	–	–	98.76
FF	280	–	–	364; –15.83	–	17.97
<b>Castings</b>						
EP	174	188; –1.09	335; –9.69	371; –10.43	–	10.18
EP/APP	175	159; –0.77	319; –9.22	369; –2.52	–	20.28
EP/APP/1VMT	181	181; –0.81	317; –12.25	362; –4.18	–	16.34
EP/APP/2VMT	176	161; –0.79	319; –10.12	355; –3.63	–	27.55
EP/APP/5VMT	204	178; –0.65	319; –11.58	358; –2.98	–	30.10
EP/APP/10VMT	225	178; –0.53	320; –11.48	361; –2.46	–	37.21
<b>Laminates</b>						
EP/FF	152	122; –0.89	–	365; –13.48	–	17.65
EP/FF/APP	274	111; –0.56	317; –9.53	–	–	37.15
EP/FF/APP/1VMT	253	116; –0.64	318; –10.23	–	–	27.70
EP/FF/APP/2VMT	271	125; –0.51	321; –9.72	–	–	28.34
EP/FF/APP/5VMT	272	149; –0.37	320; –9.91	–	–	39.07
EP/FF/APP/10VMT	271	139; –0.42	319; –9.81	–	–	36.95

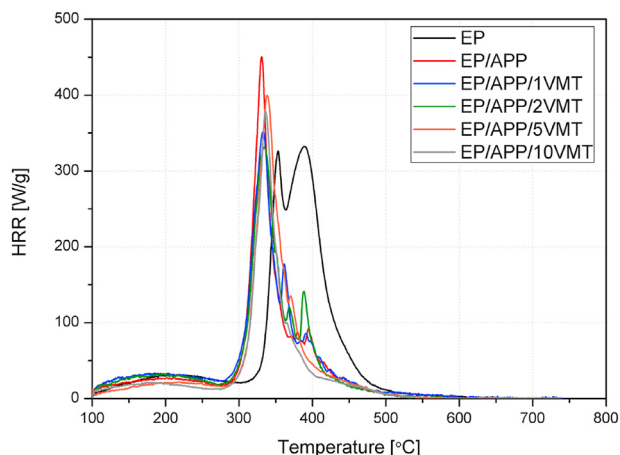


Fig. 7. Selected HRR vs. temperature curves for non-reinforced EP, EP/APP, and EP/APP/VMT composites.

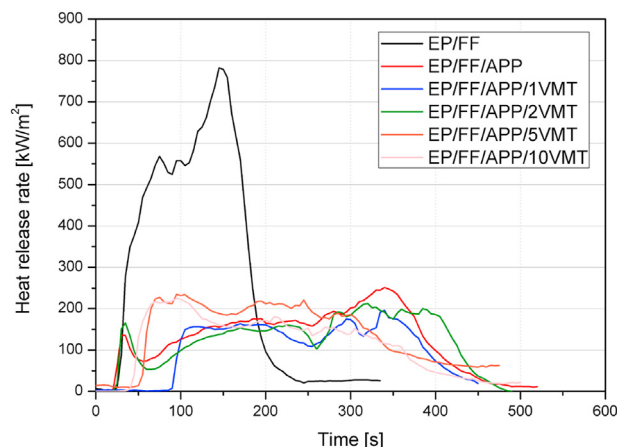


Fig. 8. Representative curves of heat release rate curves of EP composites.

**Table 4**  
Combustion-related parameters obtained from PCFC.

Sample	$T_{pHRR}$ , °C	pHRR, W/g	THR, kJ/g	HRC, J/gK
EP	363 ± 21	353 ± 35	33.8 ± 1.3	385 ± 26
EP/APP	331 ± 1	431 ± 56	23.6 ± 0.4	470 ± 66
EP/APP/1VMT	333 ± 2	351 ± 46	23.5 ± 1.6	385 ± 52
EP/APP/2VMT	332 ± 1	329 ± 24	22.2 ± 2.0	360 ± 26
EP/APP/5VMT	336 ± 2	391 ± 43	22.6 ± 0.8	432 ± 46
EP/APP/10VMT	336 ± 2	376 ± 5	20.7 ± 1.5	407 ± 7

polymers with APP, it can still provide valuable information about flammability. As can be seen from Table 4, all parameters, including pHRR, THR, and HRC, indicate that the EP/APP/2VMT possesses a better fire-resistant effect than the unmodified epoxy resin. Due to the potential of the developed materials, they were modified by the same share of natural fibers and tested using a cone calorimeter as a comprehensive device for assessing the behavior of polymers during burning.

### 3.5.3. Cone calorimetry

Cone calorimeter tests are crucial to characterize a polymeric material's fire behavior. Several parameters such as time of ignition (TTI), peak heat release rate (pHRR), the maximum average rate of heat emission (MARHE), total heat release (THR), effective heat of combustion (EHC), specific extinction area (SEA), total smoke release (TSR) and char yield at flameout are summarized in Table 5. Figs. 8 and 10 display the heat release rate (HRR) and the total smoke release (TSR) curves of the composites over time, while the residues are shown in Fig. 9.

The heat release rate curve of resin with flax-cotton fabrics presents a peak at the end of the burning at ca. 150 s before the HRR quickly decreases, which is characteristic of non-charring samples.

**Table 5**  
Cone calorimeter results of EP composites.

Sample	TTI, s	pHRR, kW/m <sup>2</sup>	MARHE, kW/m <sup>2</sup>	THR, MJ/m <sup>2</sup>	EHC, MJ/kg	Residue, %	SEA, m <sup>2</sup> /kg
EP/FF	48 (6 <sup>a</sup> )	730 (73)	434 (45)	80 (6)	21 (3)	3 (1)	510 (10)
EP/FF/APP	27 (4)	279 (39)	182 (40)	76 (16)	23 (7)	37 (1)	406 (22)
EP/FF/APP/1VMT	55 (37)	208 (11)	133 (17)	53 (10)	17 (2)	40 (2)	383 (9)
EP/FF/APP/2VMT	56 (7)	204 (13)	130 (12)	55 (3)	17 (0)	41 (1)	400 (49)
EP/FF/APP/5VMT	62 (2)	218 (24)	163 (6)	58 (7)	18 (4)	37 (0)	479 (21)
EP/FF/APP/10VMT	52 (3)	225 (0)	157 (16)	54 (1)	15 (3)	36 (4)	486 (62)

<sup>a</sup> The values in parentheses refer to standard deviations.

The curve consists of two stages: a minor maximum (ca. 75s) and the following yielding the pHRR. In turn, all APP-containing samples revealed a protective layer effect specified by the considerable reduction in pHRR. APP induces charring so that the fuel release is reduced and causes fuel dilution because of the NH<sub>3</sub> release [81]. Therefore, the HRR curves of EP/FF/APP/VMT are characteristic of a thermally thick charring material, with, in some cases, an additional peak at the end of burning caused by the cracking of the protective layer [82]. Accordingly, the pHRR for flame retarded composites is 2.5 (EP/FF/APP) or even 3.5 times (EP/FF/APP/1VMT and EP/FF/APP/2VMT) lowered compared to EP/FF. The lowest pHRR, equal to 208 and 204 kW/m<sup>2</sup>, were obtained for EP/FF/APP/1VMT and EP/FF/APP/2VMT, respectively, so the values were independent of filler content. Similarly, the lowest MARHE was obtained for samples with lower pHRR; however, all samples with vermiculite were characterized by lowered values. MARHE is one of the critical indicators enabling flame spread evaluation. Additionally, the TTI clearly shows that EP with phosphorus-based fire retardant ignited quicker than resin without APP, while the incorporation of vermiculite changed this tendency substantially (Table 5). VMT is a well-known filler with flame-retardant effects [83–85].

VMT addition led to a significant but non-linear decline of THR, indicating incomplete combustion impacted by char formation or reduced combustion efficiency. The appearance of a char is confirmed both by the significantly increased residue values (Table 5) and by photographs of the samples after burning (Fig. 9). The analysis of the photographs confirms that the presence of 1 to 2% of vermiculite facilitated forming of a more compact structure, despite the use of growth restriction mesh for samples with intumescent flame retardants (Fig. 9). In turn, the higher content of VMT may hindered the swelling of the char during setting. Effective heat of combustion is an indicator to evaluate the efficiency of a flame retardant in terms of flame inhibition action by activity in the gas phase [86]. Since the amount of APP was the same for all



Fig. 9. Photographs of samples after cone calorimetry tests a) EP/FF, b) EP/FF/APP, c) EP/FF/APP/1VMT, d) EP/FF/APP/2VMT, e) EP/FF/APP/5VMT, f) EP/FF/APP/10VMT.

samples, more probably was the influence of the decreased resin amount, as one of the main combustible components, in favor of an inorganic filler with high thermal stability. Both carbonaceous char, working as a barrier for heat and mass transfer, and inert residue from inorganic fillers reduce fuel release, decreasing THR [87].

Fig. 9 presents the residues of the composites obtained after cone calorimeter measurements. Thin layers of flax/cotton fabrics were obtained for EP/FF, while the epoxy resin was consumed entirely during burning. In the case of EP/FF/APP with VMT, the formed char provided a barrier protecting the materials

underneath and reducing the rate of further degradation [86]. The largest-sized char with a compact structure was created in the case of composites with 1–2% vermiculite, and an increase in its content to 5% or more resulted in the formation of a carbonaceous layer of worse quality, even compared to EP/FF/APP without VMT. An effective char should be cohesive and provide an appropriate temperature gradient; therefore, increasing the VMT amount is unreasonable.

The smoke emission in fire poses a significant hazard to victims of an unexpected fire. Smoke particles hinder visibility and may

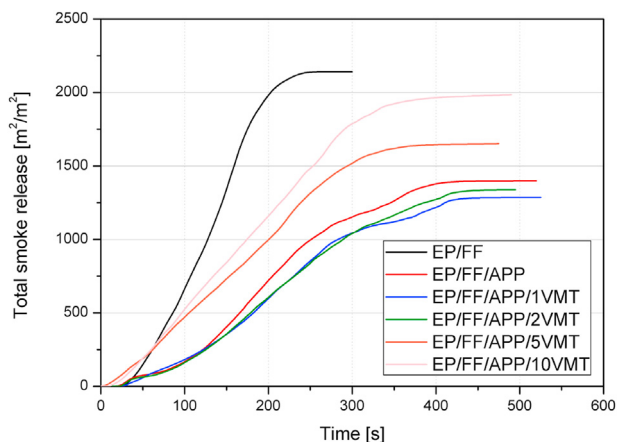


Fig. 10. Representative curves of total smoke release curves of EP composites.

retard rescue procedures due to their light-absorbing and scattering properties [88]. Furthermore, 70% of fire casualties are caused by smoke inhalation, not by flames [86]. The formation of significant size char also influenced the emission of smoke. In the case of materials forming a protective layer on the surface, some of the products of incomplete combustion were embedded or trapped in the char. Therefore, the lowest specific extinction area was noted for EP/FF/APP/1VMT and EP/FF/APP/2VMT, and the reduction achieved was 25% and 22%, respectively. A similar observation was made in the case of total smoke release (Fig. 10). The analysis of the curves showed that epoxy resin with flax/cotton fabrics reached the maximum value the fastest of all materials. Moreover, although the samples with vermiculite burned almost twice as long, none of them exceeded the TSR obtained for EP/FF during the entire duration of the measurements.

#### 4. Conclusions

The research on the hybridization of flame retardant epoxy composites modified with flax-cotton fibers and expanded vermiculite allows for finding favorable effects in the case of using low concentrations of VMT (1, 2 wt%). Introducing a fine-dispersive filler with high thermal stability and lamellar structure allowed for over 20% improvement in flexural and tensile strength and obtaining a synergistic effect of interaction with ammonium polyphosphate, leading to reduced flammability of composites. The application of the lowest content of VMT caused a reduction of the total heat release of the APP-modified composites by over 20 MJ/m<sup>2</sup>.

At the same time, it has been shown that VMT was an effective filler of APP-modified epoxy composites in the form of castings. This effect was limited when the EP/APP/VMT compositions were incorporated into laminates reinforced with natural fillers. It has been shown that the beneficial effects of the inorganic filler, both in terms of mechanical performance and flammability, have been almost completely limited by the occurrence of reactions between the natural fibers and the epoxy resin for composites with 5 and 10 wt% VMT share, causing probably by the modification of its cross-link structure.

The conducted tests conclude that it is possible to produce natural fiber-reinforced composites with limited flammability and good mechanical performance for structural lightweight and sustainable applications. Experimental works have shown the application potential of laminates made by introducing small amounts of micrometric plate-shaped filler. However, they also indicate the need for more advanced and procedurally optimized processing

methods use, such as vacuum-assisted resin transfer molding (VARTM) or resin infusion, in order to use their full potential.

#### Declaration of competing interests

The authors declare that they have no known competing financial interests or personal relationships that could have appeared to influence the work reported in this paper.

#### Acknowledgment

This research was funded by the Ministry of Science and Higher Education in Poland, allocated at Poznan University of Technology, grant number 0513/SBAD/4774.

#### Appendix A. Supplementary data

Supplementary data to this article can be found online at <https://doi.org/10.1016/j.aiepr.2023.01.005>.

#### References

- [1] P.K. Bajpai, I. Singh (Eds.), Reinforced Polymer Composites, Wiley-VCH Verlag GmbH & Co. KGaA, Weinheim, Germany, 2019, <https://doi.org/10.1002/9783527820979>.
- [2] B.T. Astrom, Manufacturing of Polymer Composites, Champan & Hall, Cheltenham, 1997.
- [3] P. Latko-Duralek, P. Bertasius, J. Macutkevicius, J. Banyas, A. Boczkowska, Fibers of thermoplastic copolyamides with carbon nanotubes for electromagnetic shielding applications, *Materials* 14 (2021) 5699, <https://doi.org/10.3390/ma14195699>.
- [4] J. Andrzejewski, S. Michalowski, Development of a new type of flame retarded biocomposite reinforced with a biocarbon/basalt fiber system: a comparative study between poly(lactic acid) and polypropylene, *Polymers* 14 (2022) 4086, <https://doi.org/10.3390/polym14194086>.
- [5] D. Matykiewicz, Hybrid epoxy composites with both powder and fiber filler: a review of mechanical and thermomechanical properties, *Materials* 13 (2020) 1802, <https://doi.org/10.3390/ma13081802>.
- [6] H.M.A. Hasan, B.A.A. Hasan, Effect of nano-kaolinite weight fraction on interfacial shear strength of fibre reinforced nanocomposite, *Compos. Theory Pract.* 22 (2022) 16–20.
- [7] D. Matykiewicz, O. Mysiukiewicz, Epoxy composites reinforced with natural fillers such as flax fiber and linseed cakes, *Polimery* 65 (2020) 828–832, <https://doi.org/10.14314/polimery.2020.11.11>.
- [8] M.J. Suriani, R.A. Ilyas, M.Y.M. Zuhri, A. Khalina, M.T.H. Sultan, S.M. Sapuan, et al., Critical review of natural fiber reinforced hybrid composites: processing, properties, applications and cost, *Polymers* 13 (2021) 3514, <https://doi.org/10.3390/polym13203514>.
- [9] D.K. Mohapatra, C.R. Deo, P. Mishra, Investigation of glass fiber influence on mechanical characteristics of natural fiber reinforced polyester composites: an experimental and numerical approach, *Compos. Theory Pract.* 22 (2022) 123–129.
- [10] M. Torres-Arellano, V. Renteria-Rodríguez, E. Franco-Urquiza, Mechanical properties of natural-fiber-reinforced biobased epoxy resins manufactured by resin infusion process, *Polymers* 12 (2020) 2841, <https://doi.org/10.3390/polym12122841>.
- [11] P. Rybiński, B. Syrek, A. Marzec, B. Szadkowski, M. Kuśmierk, M. Śliwka-Kaszyńska, et al., Effects of basalt and carbon fillers on fire hazard, thermal, and mechanical properties of EPDM rubber composites, *Materials* 14 (2021) 5245, <https://doi.org/10.3390/ma14185245>.
- [12] K. Salasińska, M. Barczewski, J. Aniśko, A. Hejna, M. Celiński, Comparative study of the reinforcement type effect on the thermomechanical properties and burning of epoxy-based composites, *J. Compos. Sci.* 5 (2021) 89, <https://doi.org/10.3390/jcs5030089>.
- [13] R. Oliwa, M. Heneczowski, M. Oleksy, H. Galina, Epoxy composites of reduced flammability, *Compos. B Eng.* 95 (2016) 1–8, <https://doi.org/10.1016/j.compositesb.2016.03.074>.
- [14] R. Oliwa, M. Oleksy, J. Czech-Polak, M. Płocińska, S. Krauze, M. Kowalski, Powder-epoxy resin/glass fabric composites with reduced flammability, *J. Fire Sci.* 37 (2019) 155–175, <https://doi.org/10.1177/0734904119831211>.
- [15] R. Ortega, M.D. Monzón, Z.C. Ortega, E. Cunningham, Study and fire test of banana fibre reinforced composites with flame retardance properties, *Open Chem* 18 (2020) 275–286, <https://doi.org/10.1515/chem-2020-0025>.
- [16] N. Wolter, V.C. Beber, A. Sandinge, P. Blomqvist, F. Goethals, M. Van Hove, et al., Carbon, glass and basalt fiber reinforced polybenzoxazine: the effects of fiber reinforcement on mechanical, fire, smoke and toxicity properties, *Polymers* 12 (2020) 2379, <https://doi.org/10.3390/polym12102379>.

- [17] P. Khalili, K.Y. Tshai, D. Hui, I. Kong, Synergistic of ammonium polyphosphate and alumina trihydrate as fire retardants for natural fiber reinforced epoxy composite, *Compos. B Eng.* 114 (2017) 101–110, <https://doi.org/10.1016/j.compositesb.2017.01.049>.
- [18] P. Khalili, K.Y. Tshai, I. Kong, Natural fiber reinforced expandable graphite filled composites: evaluation of the flame retardancy, thermal and mechanical performances, *Compos. Part A Appl. Sci. Manuf.* 100 (2017) 194–205, <https://doi.org/10.1016/j.compositesa.2017.05.015>.
- [19] B. Wei, H. Cao, S. Song, Surface modification and characterization of basalt fibers with hybrid sizings, *Compos. Part A Appl. Sci. Manuf.* 42 (2011) 22–29, <https://doi.org/10.1016/j.compositesa.2010.09.010>.
- [20] F.H. Chowdhury, M.V. Hosur, S. Jeelani, Studies on the flexural and thermo-mechanical properties of woven carbon/nanoclay-epoxy laminates, *Mater. Sci. Eng.* 421 (2006) 298–306, <https://doi.org/10.1016/j.msea.2006.01.074>.
- [21] I.D.G. Ary Subagia, L.D. Tijing, Y. Kim, C.S. Kim, F.P. Vista, H.K. Shon, Mechanical performance of multiscale basalt fiber-epoxy laminates containing tourmaline micro/nano particles, *Compos. B Eng.* 58 (2014) 611–617, <https://doi.org/10.1016/j.compositesb.2013.10.034>.
- [22] G. Velmurugan, L. Natrayan, Y.S. Rao, P. Gaur, S. Sekar, R. Chebolu, et al., Influence of epoxy/nanosilica on mechanical performance of hemp/kevlar fiber reinforced hybrid composite with an ultrasonic frequency, *Adv. Sci. Technol.* 2022 (2022) 1–11, <https://doi.org/10.1155/2022/7233255>.
- [23] A. Vedernikov, Y. Nasonov, R. Korotkov, S. Gusev, I. Akhatov, A. Safonov, Effects of additives on the cure kinetics of vinyl ester pultrusion resins, *J. Compos. Mater.* 55 (2021) 2921–2937, <https://doi.org/10.1177/00219983211001528>.
- [24] Drummer Zhao, Influence of filler content and filler size on the curing kinetics of an epoxy resin, *Polymers* 11 (2019) 1797, <https://doi.org/10.3390/polym11111797>.
- [25] H. Ng, I. Manas-Zloczower, Chemorheology of unfilled and filled epoxy resins, *Polym. Eng. Sci.* 33 (1993) 211–216, <https://doi.org/10.1002/pen.760330404>.
- [26] M. Harsch, J. Karger-Kocsis, M. Holst, Influence of fillers and additives on the cure kinetics of an epoxy/anhydride resin, *Eur. Polym. J.* 43 (2007) 1168–1178, <https://doi.org/10.1016/j.eurpolymj.2007.01.025>.
- [27] [https://liliafarby24.pl/barpat1/uploads/2022/11/Informacja\\_Techniczna\\_Epidian\\_652.pdf](https://liliafarby24.pl/barpat1/uploads/2022/11/Informacja_Techniczna_Epidian_652.pdf).
- [28] <https://www.clariant.com/en/Solutions/Products/2014/03/18/16/31/Exolit-AP-422?p=1>.
- [29] A. Hejna, K. Piszcz-Karaś, N. Filipowicz, H. Cieśliński, J. Namieśnik, M. Marć, et al., Structure and performance properties of environmentally-friendly biocomposites based on poly( $\epsilon$ -caprolactone) modified with copper slag and shale drill cuttings wastes, *Sci. Total Environ.* 640–641 (2018) 1320–1331, <https://doi.org/10.1016/j.scitotenv.2018.05.385>.
- [30] M. Barczewski, O. Mysiukiewicz, A. Hejna, R. Biskup, J. Szulc, S. Michaiowski, et al., The effect of surface treatment with isocyanate and aromatic carbodiimide of thermally expanded vermiculite used as a functional filler for poly(lactide)-based composites, *Polymers* 13 (2021) 890, <https://doi.org/10.3390/polym13060890>.
- [31] M. Barczewski, O. Mysiukiewicz, D. Matykiewicz, K. Skórczewska, K. Lewandowski, J. Andrzejewski, et al., Development of polylactide composites with improved thermomechanical properties by simultaneous use of basalt powder and a nucleating agent, *Polym. Compos.* 41 (2020) 2947–2957, <https://doi.org/10.1002/pc.25589>.
- [32] M. Barczewski, D. Matykiewicz, M. Szostak, The effect of two-step surface treatment by hydrogen peroxide and silanization of flax/cotton fabrics on epoxy-based laminates thermomechanical properties and structure, *J. Mater. Res. Technol.* 9 (2020) 13813–13824, <https://doi.org/10.1016/j.jmrt.2020.09.120>.
- [33] ISO 11357-1:2016: *Plastics — Differential Scanning Calorimetry (DSC) — Part 1: General Principles*, 2016.
- [34] ISO 11358-1:2022: *Plastics — Thermogravimetry (TG) of Polymers — Part 1: General Principles*, 2022.
- [35] 2012, ASTM D7309-07: *Standard Test Method for Determining Flammability Characteristics of Plastics and Other Solid Materials Using Microscale Combustion Calorimetry*, 2012.
- [36] 2020, ISO 5660-1:2015: *Reaction-To-Fire Tests — Heat Release, Smoke Production and Mass Loss Rate — Part 1: Heat Release Rate (Cone Calorimeter Method) and Smoke Production Rate (Dynamic Measurement)*, 2015.
- [37] 2019, ISO 6721-1:2019: *Plastics — Determination of Dynamic Mechanical Properties — Part 1: General Principles*, 2019.
- [38] ISO 527-1:2019: *Plastics — Determination of Tensile Properties — Part 1: General Principles*, 2019.
- [39] ISO 527-4:2021: *Plastics — Determination of Tensile Properties — Part 4: Test Conditions for Isotropic and Orthotropic Fibre-Reinforced Plastic Composites*, 2021.
- [40] ISO 178:2019: *Plastics — Determination of Flexural Properties*, 2019.
- [41] ISO 868:2003: *Plastics and Ebonite — Determination of Indentation Hardness by Means of a Durometer (Shore Hardness)*, 2018.
- [42] ISO 179-2:2020: *Plastics — Determination of Charpy Impact Properties — Part 2: Instrumented Impact Test*, 2020.
- [43] F. Liu, W. Yu, Y. Wang, R. Shang, Q. Zheng, Curing kinetics and thixotropic properties of epoxy resin composites with different kinds of fillers, *J. Mater. Res. Technol.* 18 (2022) 2125–2139, <https://doi.org/10.1016/j.jmrt.2022.03.102>.
- [44] S. Mueller, E.W. Llewellyn, H.M. Mader, The rheology of suspensions of solid particles, *Proc. R. Soc. A Math. Phys. Eng. Sci.* 466 (2010) 1201–1228, <https://doi.org/10.1098/rspa.2009.0445>.
- [45] M. Barczewski, K. Salasińska, J. Szulc, Application of sunflower husk, hazelnut shell and walnut shell as waste agricultural fillers for epoxy-based composites: a study into mechanical behavior related to structural and rheological properties, *Polym. Test.* 75 (2019) 1–11, <https://doi.org/10.1016/j.polymertesting.2019.01.017>.
- [46] S.T. Cholake, M.R. Mada, R.K. Singh Raman, Y. Bai, X.L. Zhao, S. Rizkalla, et al., Quantitative analysis of curing mechanisms of epoxy resin by mid- and near-fourier transform infra red spectroscopy, *Defence Sci. J.* 64 (2014) 314–321, <https://doi.org/10.14429/dsj.64.7326>.
- [47] T. Theophanides (Ed.), *Infrared Spectroscopy - Materials Science, Engineering and Technology*, InTech, 2012, <https://doi.org/10.5772/2055>.
- [48] B. Mailhot, S. Morlat-Thérias, P.O. Bussière, J.L. Gardette, Study of the degradation of an epoxy/amine resin, 2 kinetics and depth-profiles, *Macromol. Chem. Phys.* 206 (2005) 585–591, <https://doi.org/10.1002/macp.200400394>.
- [49] A. Marzec, B. Szadkowski, J. Rogowski, P. Rybiński, W. Maniukiewicz, Novel eco-friendly hybrid pigment with improved stability as a multifunctional additive for elastomer composites with reduced flammability and pH sensing properties, *Dyes Pigments* 186 (2021), <https://doi.org/10.1016/j.dyepig.2020.108965>.
- [50] J. Aniśko, M. Barczewski, A. Piasecki, K. Skórczewska, J. Szulc, M. Szostak, The relationship between a rotational molding processing procedure and the structure and properties of biobased polyethylene composites filled with expanded vermiculite, *Materials* 15 (2022) 5903, <https://doi.org/10.3390/ma15175903>.
- [51] R.B.L. Hanken, R.R. Arimatéia, G.M.G. Farias, P. Agrawal, L.N.L. Santana, D.M.G. Freitas, et al., Effect of natural and expanded vermiculite clays on the properties of eco-friendly biopolyethylene-vermiculite clay biocomposites, *Compos. B Eng.* 175 (2019), 107184, <https://doi.org/10.1016/j.compositesb.2019.107184>.
- [52] J. Ni, L. Chen, K. Zhao, Y. Hu, L. Song, Preparation of gel-silica/ammonium polyphosphate core-shell flame retardant and properties of polyurethane composites, *Polym. Adv. Technol.* 22 (2011) 1824–1831, <https://doi.org/10.1002/pat.1679>.
- [53] F. Fraga, E.C. Vazquez, E. Rodriguez-Nunez, J.M. Martinez-Ageitos, Curing kinetics of the epoxy system diglycidyl ether of bisphenol A/isophoronediamine by Fourier transform infrared spectroscopy, *Polym. Adv. Technol.* 19 (2008) 1623–1628, <https://doi.org/10.1002/pat>.
- [54] R. Acosta Ortiz, A.E. García Valdez, D. Hernández Cruz, G. Nestoso Jiménez, A.I. Hernández Jiménez, J.G. Téllez Padilla, et al., Highly reactive novel bio-based cycloaliphatic epoxy resins derived from nopol and a study of their cationic photopolymerization, *J. Polym. Res.* 27 (2020) 144, <https://doi.org/10.1007/s10965-020-02106-4>.
- [55] P. Maity, S. Kasisomayajula, V. Parameswaran, S. Basu, N. Gupta, Improvement in surface degradation properties of polymer composites due to pre-processed nanometric alumina fillers, *IEEE Trans. Dielectr. Electr. Insul.* 15 (2008) 63–72, <https://doi.org/10.1109/T-DEL.2008.4446737>.
- [56] K. Salasińska, M. Celiński, M. Barczewski, M.K. Leszczyński, M. Borucka, P. Kozikowski, Fire behavior of flame retarded unsaturated polyester resin with high nitrogen content additives, *Polym. Test.* 84 (2020), 106379, <https://doi.org/10.1016/j.polymertesting.2020.106379>.
- [57] J.M. Salla, J.L. Martín, Dynamic, isothermal and residual heats of curing of an unsaturated polyester resin, *Thermochim. Acta* 126 (1988) 339–354, [https://doi.org/10.1016/0040-6031\(88\)87279-4](https://doi.org/10.1016/0040-6031(88)87279-4).
- [58] G.C. Papanicolaou, V. Kostopoulos, L.C. Kontaxis, E. Kollia, A. Kotrotsos, A comparative study between epoxy/Titania micro- and nanoparticle composites thermal and mechanical behavior by means of particle-matrix interphase considerations, *Polym. Eng. Sci.* 58 (2018) 1146–1154, <https://doi.org/10.1002/pen.24668>.
- [59] S.-J. Park, F.-L. Jin, J.-R. Lee, Synthesis and thermal properties of epoxidized vegetable oil, macromol, *Rapid Commun* 25 (2004) 724–727, <https://doi.org/10.1002/marc.200300191>.
- [60] S.-J. Park, F.-L. Jin, C. Lee, Preparation and physical properties of hollow glass microspheres-reinforced epoxy matrix resins, *Mater. Sci. Eng.* 402 (2005) 335–340, <https://doi.org/10.1016/j.msea.2005.05.015>.
- [61] S.N. Raja, S. Basu, A.M. Limaye, T.J. Anderson, C.M. Hyland, L. Lin, et al., Strain-dependent dynamic mechanical properties of Kevlar to failure: structural correlations and comparisons to other polymers, *Mater. Today Commun.* 2 (2015) e33–e37, <https://doi.org/10.1016/j.mtcomm.2014.11.002>.
- [62] D. Haines, J.-M. Leban, C. Herbe, Determination of Young's modulus for spruce, fir and isotropic materials by the resonance flexure method with comparisons to static flexure and other dynamic methods, *Wood Sci. Technol.* 30 (1996), <https://doi.org/10.1007/BF00229348>.
- [63] F. da C. Garcia Filho, F.S. da Luz, M.S. Oliveira, A.C. Pereira, U.O. Costa, S.N. Monteiro, Thermal behavior of graphene oxide-coated piassava fiber and their epoxy composites, *J. Mater. Res. Technol.* 9 (2020) 5343–5351, <https://doi.org/10.1016/j.jmrt.2020.03.060>.
- [64] M. Sandomierski, T. Buchwald, M. Barczewski, A. Voelkel, Improvement of mechanical properties of silica/phenolic composites and abrasive tools by modification of filler using diazonium salt with hydroxymethyl groups, *Polym. Test.* 75 (2019) 373–379, <https://doi.org/10.1016/j.polymertesting.2019.03.006>.
- [65] M. Palumbo, G. Donzella, E. Tempesti, P. Ferruti, On the compressive elasticity of epoxy resins filled with hollow glass microspheres, *J. Appl. Polym. Sci.* 60 (1996) 47–53, [https://doi.org/10.1002/\(SICI\)1097-4628\(19960404\)60:1<47::AID-APP6>3.0.CO;2-V](https://doi.org/10.1002/(SICI)1097-4628(19960404)60:1<47::AID-APP6>3.0.CO;2-V).
- [66] O. Mysiukiewicz, P. Kosmela, M. Barczewski, A. Hejna, Mechanical, thermal and rheological properties of polyethylene-based composites filled with

- micrometric aluminum powder, *Materials* 13 (2020) 1242, <https://doi.org/10.3390/ma13051242>.
- [67] T. Sterzyński, J. Tomaszewska, J. Andrzejewski, K. Skórczewska, Evaluation of glass transition temperature of PVC/POSS nanocomposites, *Compos. Sci. Technol.* 117 (2015) 398–403, <https://doi.org/10.1016/j.compscitech.2015.07.009>.
- [68] I. Amar, H. Brahim, A. Chouaib, B. Boudjema, B. Ibtissem, Rheological behavior of the epoxy resin loaded with the pozzolan, *J. Mater. Sci. Eng. A*. 7 (2012) 519.
- [69] B. Wang, Z. Yin, Y. Zhang, P. Jia, R. He, F. Yu, et al., Robust flame-retardant, super mechanical laminate epoxy composites with tunable electromagnetic interference shielding, *Mater. Today Phys.* 26 (2022), 100724, <https://doi.org/10.1016/j.mtphys.2022.100724>.
- [70] T. Srinivasan, G. Suresh, K. Santhoshpriya, C.T. Chidambaram, K.R. Vijayakumar, A. Abdul Munaf, Experimental analysis on mechanical properties of banana fibre/epoxy (particulate) reinforced composite, *Mater. Today Proc.* 45 (2021) 1285–1289, <https://doi.org/10.1016/j.matpr.2020.05.103>.
- [71] G. Pritchard, Q. Yang, Microscopy of impact damage in particulate-filled glass-epoxy laminates, *J. Mater. Sci.* 29 (1994) 5047–5053, <https://doi.org/10.1007/BF01151095>.
- [72] G.C. Stevens, M.J. Richardson, Factors influencing the glass transition of DGEBA-anhydride epoxy resins, *Polymer* 24 (1983) 851–858, [https://doi.org/10.1016/0032-3861\(83\)90203-3](https://doi.org/10.1016/0032-3861(83)90203-3).
- [73] Q.J. Singh, G. Rajamurugan, Importance of WCFC particle on the mechanical and tribological performance of flax/hemp epoxy composite, *Part. Sci. Technol.* (2022) 1–13, <https://doi.org/10.1080/02726351.2022.2066586>.
- [74] V. Švehlová, E. Polouček, About the influence of filler particle size on toughness of filled polypropylene, *Angew. Makromol. Chem.* 153 (1987) 197–200, <https://doi.org/10.1002/apmc.1987.051530115>.
- [75] M.E. Kazemi, L. Shanmugam, Z. Li, R. Ma, L. Yang, J. Yang, Low-velocity impact behaviors of a fully thermoplastic composite laminate fabricated with an innovative acrylic resin, *Compos. Struct.* 250 (2020), 112604, <https://doi.org/10.1016/j.compstruct.2020.112604>.
- [76] D. Matykiewicz, M. Barczewski, M.S. Mousa, M.R. Sanjay, S. Siengchin, Impact strength of hybrid epoxy–basalt composites modified with mineral and natural fillers, *ChemEngineering* 5 (2021) 56, <https://doi.org/10.3390/chemengineering5030056>.
- [77] S.P.B. Sousa, M.C.S. Ribeiro, P.R.O. Nóvoa, C.M. Pereira, A.J.M. Ferreira, Mechanical behaviour assessment of unsaturated polyester polymer mortars filled with nano-sized Al<sub>2</sub>O<sub>3</sub> and ZrO<sub>2</sub> particles, *Ciência Tecnol. Dos Mater.* 29 (2017) e167–e171, <https://doi.org/10.1016/j.ctmat.2016.08.002>.
- [78] J. Naveen, M. Jawaid, E.S. Zainudin, M.T.H. Sultan, R. Yahaya, M.S. Abdul Majid, Thermal degradation and viscoelastic properties of Kevlar/Cocos nucifera sheath reinforced epoxy hybrid composites, *Compos. Struct.* 219 (2019) 194–202, <https://doi.org/10.1016/j.compstruct.2019.03.079>.
- [79] G. Schinazi, E.J. Price, D.A. Schiraldi, Fire testing methods of bio-based flame-retardant polymeric materials, in: *Bio-Based Flame-Retardant Technol.* *Polym. Mater.*, Elsevier, 2022, pp. 61–95, <https://doi.org/10.1016/B978-0-323-90771-2.00009-2>.
- [80] C. Hamciuc, T. Vlad-Bubulac, D. Serbezeanu, A.-M. Macsim, G. Lisa, I. Anghel, et al., Effects of phosphorus and boron compounds on thermal stability and flame retardancy properties of epoxy composites, *Polymers* 14 (2022) 4005, <https://doi.org/10.3390/polym14194005>.
- [81] P. Müller, B. Schartel, Melamine poly(metal phosphates) as flame retardant in epoxy resin: performance, modes of action, and synergy, *J. Appl. Polym. Sci.* 133 (2016), <https://doi.org/10.1002/app.43549> n/a-n/a.
- [82] A. Battig, N.A.-R. Fadul, D. Frasca, D. Schulze, B. Schartel, Multifunctional graphene nanofiller in flame retarded polybutadiene/chloroprene/carbon black composites, *E-Polymers* 21 (2021) 244–262, <https://doi.org/10.1515/epoly-2021-0026>.
- [83] Q. Ren, Y. Zhang, J. Li, J.C. Li, Synergistic effect of vermiculite on the intumescent flame retardance of polypropylene, *J. Appl. Polym. Sci.* 120 (2011) 1225–1233, <https://doi.org/10.1002/app.33113>.
- [84] F. Wang, Z. Gao, M. Zheng, J. Sun, Thermal degradation and fire performance of plywood treated with expanded vermiculite, *Fire Mater.* 40 (2016) 427–433, <https://doi.org/10.1002/fam.2297>.
- [85] K. Sałasińska, M. Kirpluks, P. Cabulis, A. Kovalovs, E. Skukis, P. Kozikowski, et al., Experimental investigation of the mechanical properties and fire behavior of epoxy composites reinforced by fabrics and powder fillers, *Processes* 9 (2021) 738, <https://doi.org/10.3390/pr9050738>.
- [86] Y.Y. Chan, C. Ma, F. Zhou, Y. Hu, B. Schartel, Flame retardant flexible polyurethane foams based on phosphorous soybean-oil polyol and expandable graphite, *Polym. Degrad. Stabil.* 191 (2021), 109656, <https://doi.org/10.1016/j.polymdegradstab.2021.109656>.
- [87] B. Schartel, T.R. Hull, Development of fire-retarded materials—interpretation of cone calorimeter data, *Fire Mater.* 31 (2007) 327–354, <https://doi.org/10.1002/fam.949>.
- [88] J. Giebutowicz, M. Rużycka, P. Wroczynski, D.A. Purser, A.A. Stec, Analysis of fire deaths in Poland and influence of smoke toxicity, *Forensic Sci. Int.* 277 (2017) 77–87, <https://doi.org/10.1016/j.forsciint.2017.05.018>.